Review

Effect of Temperature and Humidity on the Performance Factors of a 15-W Proton Exchange Membrane Fuel Cell

Dien Minh Vu, Binh Hoa Pham, Duc Pham Xuan*, Dung Nguyen Dinh** and Vinh Nguyen Duy*,†

Center for Automotive Technology and Driving Training, Hanoi University of Industry, Hanoi 100000, Vietnam
*Faculty of Vehicle and Energy Engineering, Phenikaa University, Hanoi 100000, Vietnam
**Faculty of Mechanical Engineering and Mechatronics, Phenikaa University, Hanoi 100000, Vietnam

Abstract

Fuel cells are one of the renewable energy sources that have sparked a lot of scientific attention for solving problems related to the energy crisis and environmental pollution. One of the most crucial subjects concerning the utilization of fuel cells is modeling. Therefore, an analytical steady-state and dynamic fuel cell model was described in this study. The parameter for the identification process was investigated, and the MATLAB/Simulink implementation was demonstrated. A 15-W proton exchange membrane fuel cell was used to apply the suggested modeling methodology. Comparing experimental and simulation findings indicated that the model error was constrained to 3%. This study showed that temperature and humidity affect fuel cell performance.

Keywords: Proton exchange membrane, Temperature control, Humidity control, Electrochemical reactions, Liquid phase

1. Introduction

Globally, there is a lot of interest in hydrogen fuel cell technology as a reliable source of renewable energy[1-5]. A global focus on renewable energy has emerged as a means of addressing global warming as a result of natural disasters and fuel shortages. These parameters are ideal for fuel cell technology[6-8]. New research may help improve fuel cells' performance, endurance, cost-effectiveness, and limitations. A proton exchange membrane fuel cell (PEMFC)'s performance might be impacted by a variety of causes. There are many variables, including the load current, temperature, relative humidity, membrane thickness, membrane-active area, active electrode area, corrosion, purity, pressure, concentration of hydrogen fuel, maintenance of water inside the cell, pressure in the electrode in particular on both sides of the membrane, *etc.*[9-11]. The fuel cell voltage is lower than it was due to activation, ohmic, and concentration losses. Two important criteria for PEMFC operation are the humidity level and the temperature. Proton exchange, water generation, and electrochemical reaction are all impacted by a fuel cell's temperature fluctuation. Two sides make up the bipolar plate. The fuel cell's temperature is maintained by an external water flow on one side and a gas flow channel on the other. The reaction process is accelerated by increasing current density. In addition, the fuel cell produces heat proportionate to the reaction's rate. The proton exchange membrane at the plate's outer portion dries out due

to the temperature increase. In the fuel cell, the density of the electron flow rate also decreases over time. When sufficient gas is provided, the electron flow's density is higher. Another crucial element is the current distribution, which is inversely related to the density of the electron flow rate. The increasing reactant flow rate produces a consistent current flow. The proton exchange membrane will operate worse with improper thermal energy.

Because of the low working temperatures and the unique features of the membrane utilized in the PEMFC, another key difficulty impacting PEMFC operation is water management depending on the temperature operation[1,12]. The fuel must be soaked with water to prevent the polymer barrier from drying out. However, excess water may condense into a liquid phase, causing flooding in the cathode gas diffusion layer, and preventing oxygen from reaching the catalyst layer, resulting in fuel cell voltage and performance losses. A high-temperature PEMFC operating at temperatures of about 373-473 K has recently been created to overcome the abovementioned difficulty. Water movement inside the PEMFC is simplified due to the high-temperature operation, and electrochemical reaction rates at the anode and cathode are boosted. Water is only present in the vapor phase at temperatures over 373 K; thus, flooding is not a concern.

On the other hand, such circumstances might cause membrane dryness and loss of membrane ionic conductivity. The efficiency of traditional PEMFCs depends on the amount of water in the membrane; hence, the performance suffers when the water content is low. Su *et al.*[11] used a three-dimensional fuel cell model to investigate the impact of operating circumstances on the performance of high-temperature PEMFC. To investigate the relationship between heat and water transport in PEMFC, Huang *et al.*[13] created a three-dimensional,

two-phase, non-isothermal model. Their simulations revealed that a linear porosity gradient in the gas diffusion layer improves capillary diffusivity, electrical conductivity, oxygen transport, and overall cell performance.

Furthermore, many studies have recently looked at the impact of relative humidity (RH) on PEMFC performance[14-16]. These studies discussed modeling, performance assessment, flow field design, membrane fabrication and modification, (membrane exchange assembly) MEA degradation, oxygen reduction reaction, and catalyst layer design. The findings showed that lowering relative humidity impacts fuel cell performance by increasing membrane resistance, decreasing proton activity in catalyst layers, lowering Pt utilization, lowering electrode kinetics, and increasing gas mass transfer resistance. Although part of the literature analyses the RH impact in high-temperature PEMFCs, most of these investigations focus on low-temperature PEMFC. RH may still substantially affect performance in a PEMFC operating at 120 °C.

The influence of stoichiometry, reservoirs and fuel dilution on the dynamic behavior of a PEMFC during load change was investigated by Kim et al.[17,18]. At a fixed intake flow rate, the steady-state current density's overshoot and undershoot behavior were observed at varied voltage change rates. Argyropoulos et al. studied the key parameters for a liquid-fed direct methanol fuel cell (DMFC) and demonstrated the effects of anode concentration, flow, and cathode pressure on the dynamic fuel cell reaction experimentally[19,20]. Xue et al. constructed a PEMFC system-level dynamic model capable of characterizing the impacts of temperature, gas flow, and capacitance, focusing on system transient behavior[29]. Shimpalee et al. reported a three-dimensional numerical simulation of a PEMFC exposed to a changing load. When the fuel cell voltage was quickly reduced from 0.7 to 0.5 V with fixed excess starting stoichiometric flow rates, the predictions exhibited transients in the current density that overshot the end state value[21]. Under widely variable working conditions, comprehensive experimental parameters are controlled and quantified in this study. Feed gas flow rates, temperatures, and relative humidity are monitored in addition to the polarisation curves. The impacts of relative humidity, temperature, and feed gas stoichiometry are explored on fuel cells' steady state and dynamic behavior. In addition, the dynamic behavior of a tiny fuel cell stack is investigated. The experimental results serve as a benchmark for fuel cell model validation.

The mathematical modeling of a PEMFC system with a resistive variable load is presented in this paper. The fuel cell electric current and voltage at different steady-state conditions were calculated using the model, which was implemented using the MATLAB Simulink program. The junction of the electric current's polarisation curve was the basis for calculating the input value for the PEMFC performance simulation.

2. The MATLAB/Simulink model

2.1. Mathematical Modeling of a PEMFC

The enormous variety of effects that must be considered makes mathematical modeling of transport phenomena in fuel cells challenging.

Numerous media, including flow channels, porous electrodes, catalytic layers, and electrolytes, are involved in flows, which are often extremely three-dimensional, non-isothermal, multiphase, multicomponent, and time-dependent. The current is often modeled in fuel cells as an independent variable that is utilized to determine the stack voltage. The external load resistance serves as a separate component in the model that affects current and voltage. Equations that connect the voltage of the fuel cell stack to its current and temperature have been used to simulate the fuel cell stack using a direct current (DC) voltage source. From the voltage source to the circuit, the stack current travels. The voltage source powers an electrical circuit consisting of a DC boost converter and a variable load. A voltage proportional-integral controller with pulse-width modulation signal control is used to operate the converter. The regulated current source models the power consumption of auxiliary components. The whole model was created using MATLAB Simulink with the Simscape tool to solve the electrical circuit in this research. Steady-state operating conditions were assumed, and the stack was represented as being isothermal and unidimensional. The blower's pressure increase and the fuel flow's pressure decrease were overlooked in favor of treating the partial pressure of the reactants as constant. In saturated circumstances, the membrane's humidity was regarded as constant. The auxiliary components' power consumption was likewise assumed to be constant. The battery and super-capacitor are not included since the model does not account for the transient circumstances during startup.

It is believed that the cell operates under steady-state conditions. The model formulation employs a one-dimensional approximation because the cell thickness is negligible relative to its other dimensions. The whole system is considered to be at a constant temperature, and the gases are assumed to be ideal and well-mixed. Since single-cell experiments often attain these conditions, the steady-state and isothermal hypotheses are true. The model needs property inputs such as water-diffusion coefficients, electro-osmotic drag coefficients, water sorption isotherms, and membrane conductivities, all determined by single-cell experimental experiments. The fuel cell temperature is believed to be well-controlled. The heat transfer should be very efficient so that the heat generated by the irreversibility of the electrochemical process, ohmic resistance, and mass transport overpotentials can be swiftly removed. Assume that the incoming gaseous temperature has been warmed to the cell's temperature. Consideration is given to fully hydrated membranes, wet gas diffusers, and saturated chamber gases. Assuming that the total gas pressure inside the gas channel is constant and the same as the pressure in the gas diffuser, the pressure fluctuation throughout the gas channel may be omitted. However, the pressure between the anode and cathode might vary.

2.2. Governing equations

For modeling purposes, the conventional fuel cell in Figure 1 is divided into four ancillaries: the anode, cathode, membrane, and voltage. The anode and cathode ancillaries simulate the molar balance of the reactant species and their partial pressures. In addition, The membrane ancillary models the water transport process and water absorption into
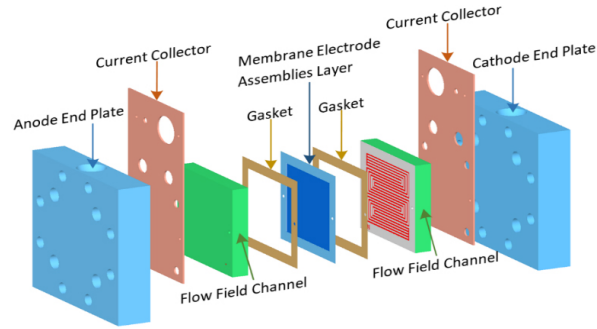
Figure 1. Schematic illustration of a computational domain for PEMFC simulation.

the membrane. The voltage auxiliary models the overpotential. The humidified hydrogen is delivered to the anode, which is oxidized following equation (1). Following equation (2), humidified oxygen/air is given to the cathode and reduced on the cathode to produce water and electricity.

The overall electrochemical reactions occurring at the reaction site may be represented as:

$$2H_2 \leftrightarrow 4H^+ + 4e^- \tag{1}$$

Therefore, the overall electrochemical reaction of the PEMFC is:

$$2H_2 + O_2 \rightarrow 2H_2O + heat + electric\ energy \tag{2}$$
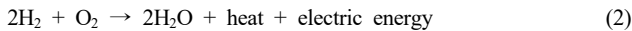
With the Gibbs free energy ΔG, the Faraday constant F, and the number of electrons n involved, it is possible to compute the theoretical maximum voltage of a PEMFC under reference conditions:

$$E_{Ref} = \frac{-\Delta_G}{nF} = 1.23\,(V) \tag{3}$$

Variations in temperature T and partial pressure of reactants p_i can be accounted for by using the Nernst-Equation as follows:

$$E_{T,P} = -\left(\frac{\Delta H}{nF} - \frac{T\Delta S}{nF}\right) + \frac{RT}{nF}\ln\left[\frac{p_{H_2}p_{O_2}^{0.5}}{p_{H_2O}}\right] \tag{4}$$

Assuming the product water is in the liquid phase and ignoring the effects of altering enthalpy ΔH and entropy ΔS, the ideal cell voltage $E_{T,P}$ may be stated as follows:

$$E_{T,P} = 1.482 - 0.000845 \times T + 0.0000431 \times T \times \ln(p_{H_2}p_{O_2}^{0.5}) \tag{5}$$

By deducting the internal voltage losses from the ideal cell voltage $E_{T,P}$ in the fuel cell model, the actual cell voltage E_{cell} is calculated.

$$E_{cell} = E_{T,P} - E_{act} - E_{ohm} - E_{con} \tag{6}$$

where E_{act} is the activation overpotential, E_{ohm} is the ohmic overvoltage, and E_{act} is the concentration overvoltage.

The activation overpotential E_{act} may be calculated using the Butler-Volmer equation as a function of current density i, exchange current density i_0, temperature T, and charge transfer coefficient α_i as mentioned in [31-33].

$$E_{act} = \frac{RT_i}{\alpha_i F}\,\mathrm{arcsin}h\left(\frac{i}{2i_{0,i}}\right) \tag{7}$$

where R denotes the universal gas constant and F the Faraday constant. Meanwhile, based on a reference value i_{ref}, a platinum electrode's exchange current density i0 may be estimated as a function of partial pressure p_i, temperature T, catalyst loading L_i, and specific area a_i.

Only the membrane resistance is considered when discussing ohmic resistances inside the cell. Ionic loss resulting from resistance to the ion passage across the membrane makes up most of the contribution to ohmic overpotential. Using Ohm's law, this membrane resistance might be represented.

$$E_{ohm} = \frac{\delta_{mem}I}{\sigma_{mem}} \tag{8}$$

where δ_{mem} is the PEM's conductivity, and σ_{mem} is the thickness of the membrane. Empirically, σ_{mem} may be described as a function of humidification and membrane water content[29,44] as:

$$\delta_{mem} = \left(0.005139\lambda - 0.00326\exp\left[1268\left(\frac{1}{T_{Ref}} - \frac{1}{303}\right)\right]\right) \tag{9}$$

where λ is the water content inside of a Nafion membrane and can be expressed as a function of water activity. Placing a hydrophilic property will produce a major determinant for membrane conductivity (σ_m) related to the membrane water content (λ) and the water activity (a_k) such that

$$\begin{aligned}\lambda &= 0.043 + 17.8a_k - 39.85a_k^2 + 36.0a_k^3 \quad (0 \leq a_k < 1)\\ &= 14.0 + 1.4(a_k - 1) \quad\quad\quad\quad\quad (1 \leq a_k \leq 3)\end{aligned} \tag{10}$$

$$a_k = \frac{x_{w,k}P(x,y)}{P_{w,k}^{sat}} \tag{11}$$

$$C_{wk} = \frac{\rho_{m,dry}}{M_{m,dry}}\lambda \tag{12}$$

Table 1. Simulation Model Parameters

Characteristic	Value
Number of cells	1
Area of the single cell	100 cm^2
External temperature	70 °C
Pressure at anode	3 atm
Pressure at cathode	3 atm
Membrane thickness	201
Membrane density	2 g/cm^3
Membrane EW	1020 g/mol

where $P_{w,k}^{sat}$ is the vapor pressure of water in stream k, $x_{w,k}$ the mole fraction of water in stream k, C_{wk} is the water vapor concentration for the anode and cathode surfaces of the MEA, $P(x,y)$ is the pressure in Pa, and $T(x,y)$ is the diffusion temperature in K.

Meanwhile, concentration overvoltage E$_{con}$ is represented by the Nernst equation as a function of temperature T, current density i, and limiting current density i_L.

$$E_{con} = \frac{RT_i}{nF} \ln\left(\frac{i_L}{i_L - i}\right) \tag{13}$$

A simplified expression of the limiting current density i_L, including the Faraday F constant, number of electrons n, diffusion coefficient D_i, gas concentration C_i, and diffusion distance δ_e can be described:

$$i_L = \frac{nFD_iC_i}{\delta_e} \tag{14}$$

$$D_i = \frac{\varepsilon}{\tau^2} \cdot (1-s)^3 \cdot D_{i,ref} \cdot \left(\frac{T}{T_{ref}}\right)^{1.5} \cdot \frac{p_{ref}}{p} \tag{15}$$

2.3. Simulation model description

As in a typical stack design, this research's model fuel cell stack includes endplate assembly models and several single cells models. Stack voltage and current are generated by connecting the outputs of separate cells in series. Accordingly, MATLAB/Simulink R2019a was used to simulate the fuel cell. The equations in this article served as the foundation for all of the models used in the simulation. Table 1 lists the fuel cell's parameters based on those of the future experimental designs.

3. Results and discussions

3.1. Model Verification

The model is verified against the experimental data operated with similar parameters. Setting the parameters for this simulation identical to those given in the reference allows the values to be compared to validate the model. For this comparison, a single cell is used. PEMFC performance was investigated by varying operational variables such as pressure, temperature, humidity, flow rate, and reacting gas. The reactive gas flow was used for single cells to form the anode and cath-
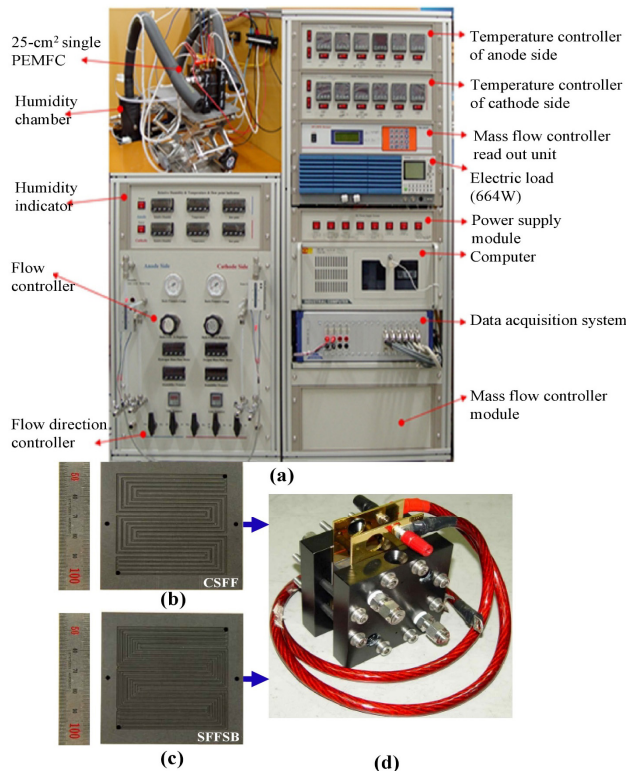

Figure 2. Experimental test setup.

ode bipolar plates in a semi-counterflow configuration.

The PEMFC performance was evaluated by measuring the polarization curve while adjusting the operating conditions, such as pressure, temperature, humidity, flow rate, and reacting gas. For single cells, the bipolar plates of the anode and the cathode were produced with the semi-counter flow of the reacting gas. The W.L. Gore & Associates PRIMEA® Series 57 MEA is sandwiched between the anode and the cathode (SIGRACET® GDLs), which has a porous structure, and a membrane and two electrodes are composed of highly dispersed carbon-supported platinum catalysts.

As a first stage, a performance test was carried out to quantify the PEMFC performance assessment, reduce physical damage to MEA, and maintain a steady state of electrical load. A 30-minute humidification method was used to hydrate the dry MEA before the performance test. The FCTESTNET performance test results prompted us to create the highest performance test process with a cell voltage of 0.01 V decrements; the test was done for 45 minutes or 132 steps per cycle.

Figure 2 shows the fabricated BPs and the front panel of the fuel cell test station in the experimental setup. The main devices include the electronic load, mass flow controller system, temperature controller, humidity and temperature measurement devices, power supply module, and data acquisition system. Each test procedure was proven in various supplemental literature and experiments[19,20]. To evaluate fuel cell performance quantitatively, a break-in procedure must be performed to minimize any physical damage to the MEA and maintain a stable electrical load.

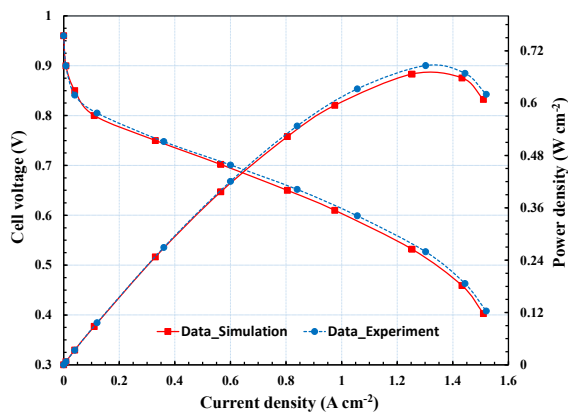Figure 3 compares the values of this simulation against the ex-

Figure 3. Comparison of simulation and experimental results.

Figure 4. Effect of temperature on the fuel cell performance.

Figure 5. Effect of relative humidity on the fuel cell performance.

perimental one. The result reveals that the simulation model's power densities are higher than the experimental one. The maximum power densities of the simulation and experiment are 0.686 W/cm², and 0.666 W/cm², respectively. The most significant difference between simulation and experimental results is approximately 3%. This difference is because the simulation model does not accurately represent the experimental parameters. However, the resulting difference is insignificant, and the simulation model is reliable for further studies.

3.2. Effect of temperature and humidity on PEEMFC performance

In this research, to study the effect of temperature on the fuel cell performance, the humidity was controlled at the value RH = 100%. Meanwhile, to evaluate the effect of humidity, the temperature value was maintained at 75 degrees Celsius.

Figure 4 shows the effect of temperature on the fuel cell characteristic. Simulation results show that when the temperature increases from 40 °C to 70 °C, the power of the fuel cell increases. This is also consistent with the results of previous studies. As the temperature increases, the loss due to activation is reduced. However, the mobility of the molecules will also increase, making it easier for the gases to reach the catalytic surface. The sum of these factors leads to an increase in capacity with increasing temperature. It can be explained that Proton exchange, water generation, and electrochemical reaction are all impacted by a fuel cell's temperature fluctuation. The fuel cell's temperature is maintained by an external water flow on one side and a gas flow channel on the other. The reaction process is accelerated by increasing current density. In addition, the fuel cell produces heat at a proportionate rate to the reaction's rate. The proton exchange membrane at the plate's outer portion dries out due to the temperature increase. In the fuel cell, the density of the electron flow rate also decreases over time. When sufficient gas is provided, the electron flow's density is higher. Another crucial element is the current distribution, which is inversely related to the density of the electron flow rate. The increasing reactant flow rate produces a consistent current flow. The proton exchange membrane will operate worse with improper thermal energy.

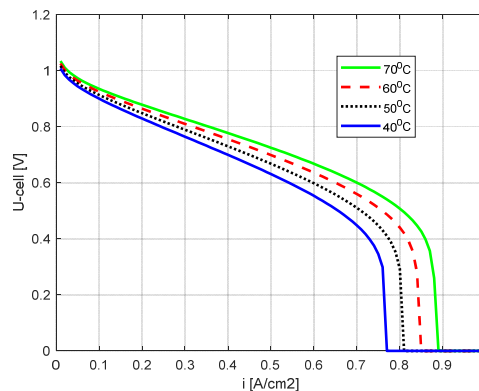The simulation results show that when the gas stream's humidity increases, the fuel cell's voltage and capacity will increase because the increased humidity will make the membrane not dry and thereby increase the proton conductivity of the membrane as in Figure 5. However, the effect was no longer apparent as humidity continued to increase. There is no difference in capacity if there is over 96% and the cathode side. Actually, the membrane's ability to exchange protons is dependent on how humid it is. The membrane's ability to hold water helps to keep it at the ideal humidity level. A sufficient amount of water must exit the fuel cell for improved performance, and the membrane must be adequately hydrated. Otherwise, the added water will cause more issues inside the fuel cell. Moreover, one of the causes of water loss in the membrane is the rise in temperature. The membrane dries out when the temperature of hydrogen fuel is kept high. As a result, less proton may move through the anode to the cathode side, which lowers the PEMFC's efficiency and electron flow. High humidity and temperatures cause a spike in membrane crossover of hydrogen gas. It is a contributing factor in PEMFC degradation. Water is created due to the electrochemical reaction following the proton exchange via the membrane. When excess water is produced, the membrane will become wet due to diffusion. A wet proton exchange membrane is absolutely necessary for proton exchange from the anode to the cathode. With the rise in temperature, the electrochemical reaction would intensify quickly and yield enough water. This water will wet the membrane, which will improve PEMFC performance.

4. Conclusions

In this research, the model of a fuel cell was built to calculate the activation loss, ohmic loss, and concentration loss based on the change in temperature and humidity. Furthermore, water transport across the membrane through osmosis, diffusion, and hydraulic osmosis was also considered. To reduce complexity and computational load, simplified correlations were used. This approach allows the model to be used in complex systems such as complete vehicle models or real-time applications. The program's code is written in MATLAB and was designed for use in the MATLAB function block inside of a Simulink model to evaluate the effect of temperature and humidity on the fuel cell performance. The result shows that the temperature and humidity dramatically affect the fuel cell operation.

References

1. V. N. Duy and H. M. Kim, Effect of gravity and gas flow direction on the operation of polymer electrolyte membrane fuel cells, *Int. J. Electrochem. Sci.*, **12**, 11833-11854 (2017).

2. N. D. Vinh and H. M. Kim, Ocean-based electricity generating system utilizing the electrochemical conversion of wave energy by ionic polymer-metal composites, *Electrochem. Commun.*, **75**, 64-68 (2017).

3. V. N. Duy, J. K. Lee, K. W. Park, and H. M. Kim, Enhancement of PEM fuel cell performance by flow control, *Mater. Sci. Forum*, **804**, 75-78 (2014).

4. V. N. Duy, K. Kim, J. Lee, J. Ahn, S. Park, T. Kim, and H.-M. Kim, Parametric simulations of optimum flow-field configuration for efficient proton exchange membrane fuel cell, *Int. J. Electrochem. Sci.*, **10**, 5842-5861 (2015).

5. T. D. Tran, S. Huang, D. H. Vu, and V. N. Duy, Effects of gas channel design on water management and on the performance of polymer electrolyte membrane fuel cells: A review, *Int. J. Electrochem. Sci.*, **13**, 10480-10495 (2018).

6. J. Lee, H.-M. Kim, T. Kim, V. N. Duy, J. Ahn, S. Park, and K. Kim, Dynamic simulations of under-rib convection-driven flow-field configurations and comparison with experiment in polymer electrolyte membrane fuel cells, *J. Power Sources*, **293**, 447-457 (2015).

7. A. Ghanbarian, M. J. Kermani, J. Scholta, and M. Abdollahzadeh, Polymer electrolyte membrane fuel cell flow field design criteria – Application to parallel serpentine flow patterns, *Energy Convers. Manag.*, **166**, 281-296 (2018).

8. J. H. Jang, H. C. Chiu, W. M. Yan, and W. L. Sun, Effects of operating conditions on the performances of individual cell and stack of PEM fuel cell, *J. Power Sources*, **180**, 476-483 (2008).

9. S. Xiong, Z. Wu, W. Li, D. Li, T. Zhang, Y. Lan, S. Ye, and S. Peng, Z. Han, Improvement of temperature and humidity control of proton exchange membrane fuel cells, *Sustainability (Switzerland)*, **13**, 1-14 (2021).

10. A. L. Lazar and S. C. Konradt, and H. Rottengruber, Open-source dynamic MATLAB/Simulink 1D proton exchange membrane fuel cell model, *Energies (Basel)*, **12**, 1-12 (2019).

11. A. Su, Y. M. Ferng, and J. C. Shih, CFD investigating the effects of different operating conditions on the performance and the char-

acteristics of a high-temperature PEMFC, *Energy*, **35**, 16-27 (2010).

12. L. Xing, M. Mamlouk, and K. Scott, A two dimensional agglomerate model for a proton exchange membrane fuel cell, *Energy*, **61**, 196-210 (2013).

13. Y. X. Huang, C. H. Cheng, X. D. Wang, and J. Y. Jang, Effects of porosity gradient in gas diffusion layers on performance of proton exchange membrane fuel cells, *Energy*, **35**, 4786-4794 (2010).

14. J. H. Jang, W. M. Yan, H. Y. Li, and Y. C. Chou, Humidity of reactant fuel on the cell performance of PEM fuel cell with baffle-blocked flow field designs, *J. Power Sources*, **159**, 468-477 (2006).

15. H. Xu, H. R. Kunz, and J. M. Fenton, Analysis of proton exchange membrane fuel cell polarization losses at elevated temperature 120 °C and reduced relative humidity, *Electrochim. Acta*, **52**, 3525-3533 (2007).

16. S. Kato, S. Yamaguchi, W. Yoshimune, Y. Matsuoka, A. Kato, Y. Nagai, and T. Suzuki, Ex-situ visualization of the wet domain in the microporous layer in a polymer electrolyte fuel cell by X-ray computed tomography under water vapor supply, *Electrochem. Commun.*, **111**, 106644 (2020).

17. S. Kim, S. Shimpalee, and J. W. van Zee, The effect of stoichiometry on dynamic behavior of a proton exchange membrane fuel cell (PEMFC) during load change,. *J. Power Sources*, **135**, 110-121 (2004).

18. S. Kim, S. Shimpalee, and J. W. van Zee, The effect of reservoirs and fuel dilution on the dynamic behavior of a PEMFC, *J. Power Sources*, **137**, 43-52 (2004).

19. M. Wang, H. Guo, and C. Ma, Dynamic response of direct methanol fuel cell under variable load, *Huagong Xuebao/Journal of Chemical Industry and Engineering (China)*, **56**, 1311-1316 (2005).

20. P. Argyropoulos, K. Scott, and W. M. Taama, Effect of operating conditions on the dynamic response of the direct methanol fuel cell, *Electrochim. Acta*, **45**, 1983-1998 (2000).

21. S. Shimpalee, W.-k. Lee, J. W. van Zee, and H. Naseri-Neshat, Predicting the transient response of a serpentine flow-field PEMFC. I. Excess to normal fuel and air, *J. Power Sources*, **156**, 355-368 (2006).

Authors

Dien Minh Vu; Ph.D., Vice Director, Center for Automotive Technology and Driving Training, Hanoi University of Industry, Hanoi 100000, Vietnam; dienvuauto@gmail.com

Binh Hoa Pham; M.Sc., Lecturer, Center for Automotive Technology and Driving Training, Hanoi University of Industry, Hanoi 100000, Vietnam; phbinh1006@gmail.com

Duc Pham Xuan; B.Sc., Faculty Member, Faculty of Vehicle and Energy Engineering, Phenikaa University, Hanoi 100000, Vietnam; duc.px19010234@st.phenikaa-uni.edu.vn

Dung Nguyen Dinh; Ph.D., Lecturer, Faculty of Mechanical Engineering and Mechatronics, Phenikaa University, Hanoi 100000, Vietnam; dung.nguyendinh@phenikaa-uni.edu.vn

Vinh Nguyen Duy; Ph.D., Team Research Leader, Faculty of Vehicle and Energy Engineering, Phenikaa University, Hanoi 100000, Vietnam; vinh.nguyenduy@phenikaa-uni.edu.vn